THE ASTROPHYSICAL JOURNAL, 190:1–10, 1974 May 15

DUST GRAINS IN A HOT GAS. I. BASIC PHYSICS

JOHN ROBERT BURKE
Department of Physics, San Francisco State University
AND
JOSEPH SILK*
Department of Astronomy, University of California, Berkeley
Received 1973 September 4

ABSTRACT

The interaction of graphite grains with a hot gas is investigated. Detailed computations, based on experimental data and simple theoretical models, are presented of the energy transfer by gas particle collisions and of the sputtering rates and grain lifetimes, as functions of gas temperature and grain radius. The electric charge on the grains is calculated, and the effect of electric forces on mechanical stability is discussed. The rate at which the gas cools by this mechanism is evaluated.

Subject heading: interstellar matter

I. INTRODUCTION

The presence of interstellar dust is observed in gaseous environments that range in temperature from $\sim 10°$ K in dense molecular clouds to $\sim 10^4$ ° K in H II regions. In Seyfert nuclei, it is probable that dust is present in regions where the gas temperature may be as high as $\sim 10^6$ ° K. More extreme environments where one might expect dust to occur include the intergalactic medium, where the temperature is usually considered to lie in the range 10^5 °–10^8 ° K, and in supernova remnants, where interstellar gas is shock-heated to temperatures as high as $\sim 10^{10}$ ° K in the earliest phases. In such regimes, gas collisions can provide an energy input to the grains exceeding that of starlight, which is ordinarily dominant in the interstellar medium.

Hitherto, little effort has been applied to obtain grain lifetimes in a hot gas. Even for dust in H II regions, the published estimates of sputtering lifetimes are largely erroneous. The related question, that of energy transfer to the grains by impinging particles, has not been seriously studied in the astrophysical literature. Yet as we shall presently demonstrate, infrared emission by grains in a hot gas can play a significant role in the energy budget of the gas, and can also provide a means of observing the gas (cf. Ostriker and Silk 1973).

The purpose of this paper is to study this mode of interaction in considerable detail. We discuss in § II the energy transfer efficiency as a function of gas temperature for grain heating by particle collisions in a hot gas. The effect of gas bombardment on the survival of the grains is studied in § III, where we give a semi-empirical relation for the sputtering yield as a function of temperature for graphite grains. In § IV we discuss the net charge acquired by the grains and its effect on their mechanical stability. In § V we illustrate the dependence of these effects on the size of the grains. These results enable us to derive sputtering rates and grain lifetimes, and to calculate the rate of gas cooling due to grain collisions, which is given in § VI. A final section summarizes our results, and indicates the effects of varying the grain composition. We defer to a subsequent paper (Silk and Burke 1974) a discussion of the applications of our results to various astrophysical environments.

* Alfred P. Sloan Research Fellow.

II. ENERGY TRANSFER

In calculating the fractional energy transfer f_i in a collision of a particle of species i with a grain, we shall consider ionization losses and excitation of lattice vibrations by impinging particles to be the primary mechanisms. We shall estimate the effect of processes more complex than two-body encounters by extrapolation of experimental data on the trapping of impinging ions by solids. For large kinetic energy of the impinging particle (about 10 keV in this context) we may neglect electron screening and use a Rutherford scattering model of the collisional excitation process. The mean energy transfer by collisions is much less than that due to ionization for the energy ranges in which the scattering approximation is valid, so that our results do not depend on the accuracy of this assumption. We obtain an estimate of the path traveled by particles, valid for high energies, by considering the path of a "typical particle" which always travels at an angle to its incident direction given by

$$\theta = N_c^{1/2}\theta_{\rm rms}\,, \tag{1}$$

where N_c is the number of encounters experienced by the particle. The differential equation for the path is then

$$\theta \cos\theta d\theta = (\theta_{\rm rms})^2 \frac{dx}{2\lambda}\,, \tag{2}$$

where θ is the angle between the particle's velocity and the x-axis, x is a coordinate measured from the entry

point in the direction of the particle's initial motion, and λ is the mean free path between encounters. For definiteness we require a model of a typical grain. In the face of severe uncertainties in grain geometry we assume a sphere of 0.1 μ radius containing some 3×10^8 atoms. This leads to a value of $\lambda \approx 1.2$ Å.

For the lowest energies one may assume a hard-sphere collision approximation. Collisional energy transfer then depends only on the ratio of particle masses α:

$$\frac{\Delta E}{E_0} \sim \frac{4\alpha}{(1+\alpha)^2} . \tag{3}$$

For intermediate and large energies, ionization is the primary energy transfer mechanism. The energy loss per centimeter by an ionizing particle is

$$\frac{dE}{dx} = \frac{2n_t Z_1^2 e^4}{m_e V_0^2} \sum_{i=z_1}^{z} \ln \frac{2m_r^2 V_0^2}{m_e I_i} . \tag{4}$$

Here n_t is the density of target atoms, Z_1 the atomic number of the incident particle, V_0 its initial velocity, m_r is the reduced mass of incident particle and electron and I_i is the ith ionization potential of the target atom. The sum is taken over those terms for which the ionization potential is less than the maximum energy the incident particle may transfer to a free electron. The ionization loss per encounter for impinging atoms is then the product of this loss rate with the mean path length.

A similar calculation may be applied to impinging electrons, but its range of validity is severely restricted by the quantum nature of the electron. For energies less than 200 eV, the de Broglie wavelength of the electron is greater than the separation of grain atoms, and a two-particle collision approximation fails completely. In this energy regime we follow Spitzer (1968) in assuming that all impinging electrons stick to the grains, so that $f_{\text{electron}} = 1$. Only for energies greater than about 10 keV does the electron wavelength become small enough to allow a classical approximation.

A significant fraction of impinging ions in the energy range from 10^3 to 10^5 eV may be completely stopped by the grains. We refer to data given by Venables (1970) on the trapping probability η of noble gas ions in tungsten. Venables notes that a hard-sphere model is capable of explaining the data for onset of trapping fairly well. Indeed, his data satisfactorily fit the following relations:

$$\begin{aligned} E_0 \Big/ \left[\frac{4\alpha}{(1+\alpha)^2}\right] &= 10^{2.10 \pm 0.05} \text{ eV} ; \\ E_{0.3} \Big/ \left[\frac{4\alpha}{(1+\alpha)^2}\right] &= 10^{2.96 \pm 0.1} \text{ eV} , \end{aligned} \tag{5}$$

where E_0 and $E_{0.3}$ are respectively the energies where $\eta = 10^{-5}$ and $\eta = 0.3$; α is the ratio of incident mass to target mass. Assuming these formulae to have generality beyond the context of noble gases striking tungsten, we find that trapping becomes significant for hydrogen on carbon at $\log_{10} E$ (eV) between 1.6 and 2.4, and for helium between 2.0 and 2.8.

Our results for energy transfer f_i are shown in figure 1. Results are plotted versus particle energy in temperature units of 10^4 ° K, so that from the temperature of ambient gas one may read off values for an average particle at that temperature. The curve

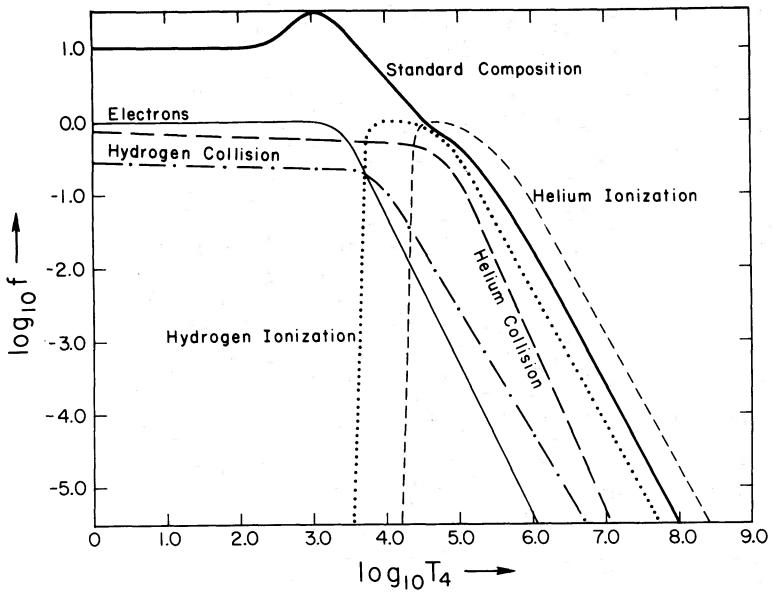

FIG. 1.—Fractional energy transfer per collision f_i for various constituents of the gas versus temperature T. The curve labeled "standard composition" is the energy transfer function f defined in § VI for a fully ionized mixture of 90 percent H, 10 percent He by number.

labeled Standard Composition is the total energy transfer function defined in § VI. We have included the effects of grain charge and particle trapping, and have assumed the gas to be a fully ionized mixture containing 10 percent helium by number.

III. SPUTTERING YIELD

In the calculation of the sputtering yield we shall again distinguish a high-energy regime in which Rutherford scattering is an adequate approximation and a low-energy region in which we may appeal to experimental data. We shall define the sputtering yield Y to be the average number of lattice atoms ejected per thermal particle impact. In the high-energy regime the incident particle passes through the grain, suffering numerous relatively small deflections and occasionally dislodging a carbon atom from the lattice. These primary carbons will themselves collide with and dislodge secondary knock-ons. In order to estimate the sputtering rate we shall assume that any carbon atom removed from the lattice within its stopping range of the grain surface is sputtered.

The spectrum of energy transfer to primary knock-ons is given by the Rutherford scattering law:

$$dP(E) = (71.2\text{ eV})\alpha Z_1^2 Z_2^2 \frac{dE}{T_4 E^2}, \qquad (6)$$

where E is the energy transferred, α is the ratio of incident to carbon mass, Z_1 and Z_2 are the atomic numbers, and T_4 measures the incident particle energy in units of 10^4 °K.

Reynolds (1966) quotes 60 eV from the work of Thompson and Wright (1965) and Lucas and Mitchell (1964) as a best available determination of the threshold energy for displacing a carbon atom. There seems to be some controversy in the literature concerning the value of the threshold, with estimates ranging as low as 25 eV (Eggen 1950); but this uncertainty has little effect on the calculation. The lower value only increases the number of knock-ons by a factor 2, and the extra particles would have a relatively short range and produce very few if any secondary knock-ons.

We also take from Reynolds the Thompson and Wright damage function $\nu(E)$ which gives the number of secondary knock-ons produced as a function of primary energy, and data for the energy loss rates of carbon ions in graphite. From these data we may compute the range R of disturbed carbons of energy E in graphite,

$$R(E) = 10^{-9.9} E^{0.8}\text{ cm (eV)}^{-0.8}. \qquad (7)$$

We estimate the spectrum of energies of the secondary knock-ons to be that corresponding to Coulomb interaction, namely, ϵ^{-2} in the range between the threshold displacement energy and the energy of the primary. This assumption may slightly overestimate the number of sputtered secondaries, for Reynolds (1966) notes that experiment does not indicate the production of tertiary knock-ons. This would indicate that the spectrum of secondaries is more bunched about low energies than we assume.

We may now write for the number of sputtered primaries:

$$\mathcal{N}_p(E_i) = \int_{E_0}^{E_{\max}} \frac{d\mathcal{N}(E)}{dx} \min\,[R(E), L(E_i)]dE, \qquad (8)$$

where $R(E)$ is the range of a primary of energy E, $L(E_i)$ is the path length of an incident particle of energy E_i, E_0 is the threshold for displacement, $E_{\max}$ is the maximum energy transfer, and $d\mathcal{N}(E)/dx$ is the number of primaries produced per unit length and is given by the mean free path length for encounters multiplied by the spectrum function dP/dE. The number of escaping secondaries is given by

$$\mathcal{N}_s(E_i) = \int_{E_0}^{E_{\max}} dE \frac{d\mathcal{N}(E)}{dx} \min\,[R(E), L(E_i)] \times \int_{E_0}^{E} \frac{\min\,[R(\epsilon), a]}{R(E)} \nu(E)\left(\frac{1}{E_0} - \frac{1}{E}\right)^{-1} \epsilon^{-2} d\epsilon, \qquad (9)$$

where ϵ is the energy of the secondary. This second expression accounts for nearly a factor 3 more sputtered particles than the first, so we shall take its value as the final result.

For low-energy incident particles, the sputtering process is sufficiently complex to baffle theoretical calculations and varies so much from situation to situation that the only practical way to obtain information is to fit a semiempirical curve to experimental data for the projectiles and targets of interest. We shall here use data obtained by Rosenberg and Wehner (1962) for He^+ on carbon. These data were obtained by exposing a spherical target, and hence are already averaged over angle of incidence. We computed a least-squares fit to these data with a formula introduced by Wehner (1958),

$$y(E) = s \frac{4\alpha}{(1+\alpha)^2}(E - E_{\text{th}}), \qquad (10)$$

finding $s = 2.1 \times 10^{-4}\text{ eV}^{-1}$ and $E_{\text{th}} = 48.8$ eV. It is of interest to note that the E_{th} obtained here agrees tolerably well with that assumed in the Thompson and Wright damage function. In order to compare these results with the high-energy computations, we have assumed that helium is, as in all other results, 10 times as efficient as hydrogen, and have divided by a factor 5 to convert results for pure helium to numbers applicable to the standard mixture of 10 percent helium.

We note that Wehner's formula may be understood in terms of a simple hard-sphere collision model (cf. Henschke 1962). We denote by X the ratio of impact parameters for which the collision transfers exactly enough energy to dislodge the target atom from the lattice to the sum of incident and target particle radii. Then X^2 is the proportion of collisions which so dislodge target atoms. We may further assume that the sputtering is proportional to X^2. One may easily show

now that for hard-sphere collisions

$$X^2 = 1 - E_b/[E4\alpha(1 + \alpha)^{-2}] = 1 - (E_{\rm th}/E)\,, \quad (11)$$

where E_b is the binding energy of the target particle and α is the ratio of incident to target masses. Thus

$$\frac{E - E_{\rm th}}{E_{\rm th}} = \frac{X^2}{1 - X^2} \approx X^2 \propto y(E)\,, \quad (12)$$

and we retrieve Wehner's energy dependence.

In addition to the above results, we show in figure 2 for comparison results by Wehner, KenKnight, and Rosenberg (1963) for H_3^+ and H_2^+ on graphite, and a result by Stuart (1961) for Hg^+ on graphite, as well as for Hg^+ on tungsten by Wehner (1958). The latter result has been used in the astrophysical literature to calibrate sputtering theories (Mathews 1969; Aannestad 1971). As discussed by Barlow (1971), the value used by Mathews for the sputtering slope s was some three orders of magnitude too large. Furthermore, it is evident both from Barlow's work and from the present comparison that one may not readily extrapolate experimental data for one target material in applications using another target material.

We have yet to consider the intermediate range of energies where electron screening limits the Rutherford scattering approximation. Wickramasinghe (1972) quotes data indicating that the incident particle energy range for which electron screening is significant is between 367 and 382 eV and quotes KenKnight and Wehner (1964) as finding a broad plateau between 1 and 5 keV in the sputtering rate for H_2^+ and H_3^+ on Fe. With these ideas in mind and assuming some electron screening out to energies where incident particles may ionize the lowest-lying electrons of carbon, we connect the high- and low-energy results as shown in figure 2.

In addition to the above mechanism, Salpeter (private communication) has suggested that shock waves set up by the passage of a particle through the grain can eject atoms from the grain surface in the vicinity of the exit point. We have applied the criterion given by Zel'dovich and Raizer (1967) for the ejection of material by unloading of a shock wave at the surface of a solid. Using the energy input calculated in § II, we find that the area over which such ejection may occur to be about 3×10^{-18} cm^2 (or 0.03A^2) at $T_4 = 10^5$. At lower temperatures, a proton does not exit a grain of radius 0.1 μ; at higher temperatures, the surface area decreases as T_4^{-3}. On the other hand, the mean surface area per atom is about 3×10^{-16} cm^2 (or 3A^2), and we infer that a rough upper limit on the sputtering yield by this mechanism amounts to

$$Y \approx 0.01(T_4/10^5)^{-3} \quad \text{for} \quad T_4 \gtrsim 10^5\,.$$

At $T_4 = 10^5$, this is approximately 50 percent of the sputtering yield computed previously. Since this effect decreases considerably more rapidly with increasing temperature than sputtering by Rutherford scattering ($Y \propto T_4^{-0.8}$), we feel justified in neglecting it.

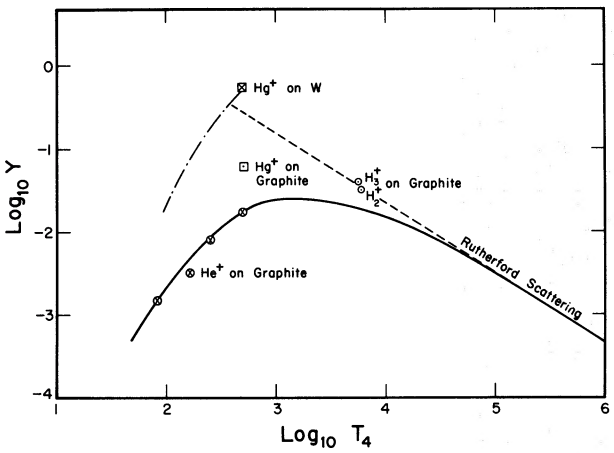

FIG. 2.—Sputtering yield per collision Y versus gas temperature T. *Solid line*, final value for Y; *dashed line*, Rutherford scattering limit; *dashed-dotted line*, application of Wehner's formula as described in the text.

IV. CHARGE ON THE GRAINS

The presence of a net electrical charge on the grains will substantially alter the cross-sections for collision with a grain of both positive gas ions and electrons. Sufficiently large charges may even give rise to forces that destroy the mechanical stability of the grains. Thus it is important to consider the processes which determine the magnitude of the charge. In this section, we consider in detail the net charge on the grain as a function of gas temperature.

a) $T_4 \lesssim 100$

At lower temperatures ($T_4 \lesssim 100$), the competing mechanisms are charge accretion by capture of impinging particles and the photoelectric effect. In the classical calculation Spitzer (1941) assumes capture by the grain of all impinging particles. In equilibrium, then, the grains will have a negative charge, so that the product of particle flux with effective cross-section is the same for both electrons and positive ions. Spitzer finds the resulting potential U to be given by

$$\psi \equiv |eU/kT| = 2.5\,, \quad (13)$$

and the ratio of effective to geometrical cross-sections for protons is $Q_{\rm coll} \equiv 1 + \psi$.

The effect of photoemission has been considered by Pecker (1971) and Watson (1972), both of whom find a positive net charge for grains in H II region.

In a more recent discussion, Feuerbacher, Willis, and Fitton (1973) conclude that graphite grains tend to be negatively charged except in the vicinity of the exciting star. In fact, the photoemission depends on a constant interstellar ultraviolet flux together with an ultraviolet photon flux emitted locally by the hot gas that decreases with temperature above 10^5 ° K. Since the collision rates important for the accretion effect increase with temperature, photoemission is probably not significant

for the temperature range of interest in the present paper.

To obtain the equilibrium grain charge, we may set the net rate of charge acquisition by a grain equal to zero:

$$\sigma_g n \frac{2}{\pi^{1/2}} \left(\frac{2kT}{m_p}\right)^{1/2} \left[\left(\frac{m_p}{m_e}\right)^{1/2} e^{-\psi} - (1 + \psi)\right] - \langle Fy \rangle \sigma_g = 0 . \quad (14)$$

Here F denotes the ultraviolet photon flux impinging upon a grain, and y the photoelectric yield, integrated over the incident photon spectrum. We can estimate the critical value of F (and therefore the ultraviolet photon flux) required for charge accretion to overcome photoemission by setting $\psi = 0$. This yields

$$\langle yF \rangle_{\rm crit} \simeq n \left(\frac{2k}{m_e}\right)^{1/2} \frac{2}{\pi^{1/2}} ,$$

or

$$\langle F_{\rm crit} \rangle \simeq 6 \times 10^7 n T_4^{1/2} \langle y \rangle^{-1} \, {\rm cm}^{-2} \, {\rm s}^{-1} . \quad (15)$$

This may be compared with the typical value calculated by Feuerbacher *et al.* (1973) for a graphite particle in Habing's (1968) radiation field of $\langle yF \rangle_{\rm ism} \approx 3 \times 10^5$ electrons cm^{-2} s^{-1} in the range 10–13.6 eV. A characteristic value of $\langle y \rangle$ for graphite in this energy range is about 0.01.

We can also compare $F_{\rm crit}$ with the rate of photoemission due to ultraviolet radiation by the local hot gas. For an emission measure $E_m \equiv n^2 R$, where n is the particle density and R the dimension of the emitting region in parsecs, we obtain

$$\langle F_{\rm gas} \rangle \approx 600 E_m T_4^{1/2} \alpha \, {\rm cm}^{-2} \, {\rm s}^{-1} , \quad (16)$$

where α is the temperature-dependent ratio of the actual gas cooling rate to its bremsstrahlung emissivity. For example, α increases from unity at $T \gtrsim 5 \times 10^6$ ° K to a maximum of ~ 1000 at $\sim 2 \times 10^5$ ° K, for a gas containing cosmical abundances of the heavier elements (Cox and Tucker 1969).

In order to illustrate the effects of photoemission on the grain charge, we show in figure 3 the solution to equation (12), for two cases, corresponding to (A) $\langle F \rangle \ll \langle F_{\rm crit} \rangle$, and (B) $\langle F \rangle = 10^9 \langle y \rangle^{-1}$ cm^{-2} s^{-1}.

b) $10^{3.8} \gtrsim T_4 \gtrsim 10^2$

At high temperatures ($T_4 \gtrsim 100$), the charges demanded by Spitzer's model will produce electric fields and field emission currents at the surface of the grain which will limit further buildup of grain charge. Assuming that the primary emission comes from the valence band, we may apply the Fowler-Nordheim equation (Gomer 1961) for the field emission current:

$$i = \frac{4}{3} \frac{16\pi m e (\mu/\phi)^{1/2}}{h^3 (\phi + \mu) b^2} F^2 \exp\left(-b\phi^{3/2}/F\right) , \quad (17)$$

where ϕ and μ are the work function and Fermi level, respectively; F is the electric field at the surface; and b

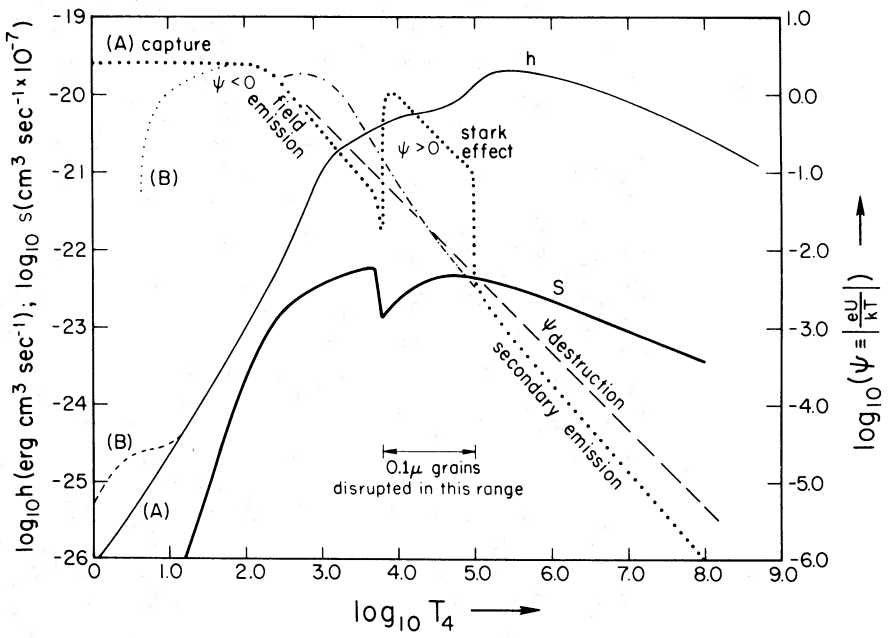

FIG. 3.—Grain charge parameter $\psi \equiv |eU/kT|$ versus temperature T. Curve (*A*), negligible photoemission; curve (*B*), significant photoemission, as defined in text. The dotted curve is the larger of the values of ψ computed from Stark effect and secondary emission limits. The charge required for mechanical disruption of the grains is $\psi_{\rm destruction}$. The collisional energy input for unit density h and sputtering rate for unit density s are computed by ignoring any disruption of the grains.

is calculated from a WKB approximation to the electron wave function in the barrier at the grain surface. After Watson (1972) we take $\phi \approx 10$ eV.

If we assume the grains to be spheres 0.1 μ in radius and let N be the number of excess electrons on the grain, we find

$$F = 1.44 \times 10^3 \mathrm{N\ Volts\ cm^{-1}},$$

$$b = 7.68 \times 10^7\ \mathrm{Volts\ cm^{-1}\ eV^{-3/2}}.$$

If we now assume Spitzer's model for the grain charge, we have $\mathrm{N} \simeq 1.5 \times 10^2 T_4$, and

$$\frac{1}{\mathrm{N}}\frac{d\mathrm{N}}{dt} \sim -10^{24} T_4 \exp\left(-3.6 \times 10^2 \phi^{3/2}/T_4\right) \mathrm{s}^{-1}. \quad (18)$$

The corresponding rate for accretion is

$$\frac{1}{\mathrm{N}}\frac{d\mathrm{N}}{dt} = \frac{1}{\mathrm{N}} n e^{-2.5}\left(\frac{8kT}{\pi m_e}\right)^{1/2} \pi r_g^2 \sim 10^{-5} n T_4^{1/2}\,\mathrm{s}^{-1}. \quad (19)$$

Equating these two rates gives a temperature $T_4 \simeq 160$. Since the exponential dependence of the field emission current is extremely rapid, we may assume that the charge on the grains never becomes more negative than that predicted by Spitzer's method for $T_4 = 160$.

c) $T_4 \gtrsim 10^{3.8}$

For temperatures in the range $T_4 \gtrsim 10^{3.8}$ the energy transfer fraction for electrons has decreased to less than 10 percent (fig. 1). The primary cause of this decrease is that the range of electrons against ionization losses in carbon is larger than the grain radius (0.1 μ) at these temperatures. Thus we may no longer maintain the assumption that impinging electrons are captured. On the other hand, it is just at the lower range of these temperatures that the capture of positive charges is most efficient.

Secondary electron emission should also become important at higher temperatures, although extrapolation of experimental data (e.g., Bruining 1938 for incident energies $\lesssim 10^3$ eV) might seem to indicate otherwise. These experiments consider back-scattered electrons which can escape, once dislocated by the incident electron, only by undergoing subsequent collisions that reverse their direction. Most of the dislocated (ionized) electrons are reabsorbed by the material. However, when the range of the electrons is larger than the thickness of the material, for grains at the temperatures we are considering, nearly all ionized electrons may escape, and this mechanism becomes important.

Thus, capture of positive charges and secondary electron emission may be expected to accumulate a powerful positive charge on the grains. One might expect this to result in a cloud of electrons bound to the grain by Coulomb forces. However, we can easily show that since the Debye shielding length in the interstellar plasma is on the order of the grain separation, the positive charging does not substantially affect the electron distribution.

Limits on the positive grain charge are set when the resulting electric fields can reeject captured positive nuclei, and restrain the escape of secondary electrons. A different limit is set when electric stresses on the grain overcome its tensile strength and shatter the grain. We consider below which limit in fact applies.

i) *Stark Effect*

Captured positive nuclei will be exposed to a density $n_\pi \sim 3 \times 10^{23}\ \mathrm{cm^{-3}}$ of π electrons which move more or less freely through the carbon lattice, and thus will tend to recombine in a time of order $\tau_R \sim 1/\alpha n_\pi \sim 3 \times 10^{-13}$ s, where α is the recombination coefficient appropriate to a grain temperature of $\sim 100°$ K. Since this time is very much shorter than the transit time of a thermalized particle across the grain, we must expect that captured particles will certainly recombine.

Near the surface of a highly charged grain, however, electric fields will act to reionize the captured particles by allowing tunneling of bound electrons in the direction opposite to the electric field. A rough estimate, applying the WKB method in a one-dimensional approximation, gives for the dissociation rate N_d:

$$\frac{dN_d}{dt} = \lambda\beta \mathrm{N}\left(\frac{Z^4 e^2}{16 m a_0^3}\right)^{1/2} \exp\left[-\left(\frac{m}{\hbar^2}\right)^{1/2} \frac{a e^3 Z^3}{a_0^{3/2}\psi kT}\right]$$

where γ and β are correction factors due to the distribution of charge in the grain and for spherical geometry, respectively; a_0 is the Bohr radius; and Z is the nuclear charge. The factor γ is the fraction of recombined particles sufficiently close to the grain surface to escape after dissociation. The correction for spherical geometry arises because the barrier may be penetrated only in directions close to that of the electric field and β is the fraction of solid angle for which this condition holds.

To find the value of ψ to which this "Stark effect" can limit the charge, we set the dissociation rate equal to the rate of capture of incoming charges:

$$(8kT/\pi m_p)^{1/2} e^{-\psi} \pi a^2 n\ \mathrm{s^{-1}}.$$

We finally obtain an equation for ψ,

$$\psi - \frac{6 \times 10^9 Z^3 a}{\psi T_4} - \ln\psi = \ln\left(7.4 \times 10^{-20} Z^{-2} T_4^{-1/2}\right), \quad (20)$$

where we have taken $\beta = \gamma = 0.1$ and $n = 1\ \mathrm{cm^{-3}}$; the results which are shown in figure 3 are fairly insensitive to these parameters. The "Stark effect" ceases to be important for $T_4 \gtrsim 10^{5.0}$ as shown in the figure because nuclei of such energies are no longer captured by the grain.

ii) *Secondary Emission*

To obtain an estimate of the secondary emission rate we shall appeal once again to Rutherford scattering theory. The ionization potentials of carbon are small compared with the incident energies we are considering; moreover, the de Broglie wavelengths of the incident electrons are much less than the impact parameters of interest. Thus quantum-mechanical

effects will not be important. Indeed, an approximate calculation using formulae for scattering of electrons by atoms (Mott and Massey 1933) gives a slightly different energy dependence of the total cross-section for ejection of electrons from the grain but does not alter the qualitative result.

From Rutherford scattering theory, we obtain the impact parameter for which energy transferred to the target electron is sufficient to remove it from the positively charged grain:

$$b = \frac{e^2}{6kT}\left(\frac{3}{2\psi} - 1\right)^{1/2} . \tag{21}$$

Thus the expected number of electrons ejected per impacting electron is

$$N_{ej} \sim \pi b^2 a\nu \sim \frac{10^9}{\psi T_4^{\,2}}\left(1 - \frac{2\psi}{3}\right) , \tag{22}$$

where $\nu \sim 0.3$ Å^{-3} is the total electron density in the grain.

Clearly an upper limit of $\psi \sim 3/2$ is established by the kinematics of energy transfer ($b = 0$). The only process tending toward a lower limit is removal of positive charges by sputtering. If we assume that each sputtered carbon nucleus carries away only its two innermost electrons, then the equilibrium equation for this process is

$$4Y\pi a^2 V_p e^{-\psi} = \pi a^2 V_e N_{ej}(1 + \psi) , \tag{23}$$

which reduces to

$$\frac{\psi e^{-\psi}}{(1 + \psi)(1 - \frac{2}{3}\psi)} \simeq 10^{10} a Y^{-1} T_4^{-2} . \tag{24}$$

The solution to this equation is plotted in figure 3 as a dashed-dotted line.

iii) *Mechanical Disruption*

If we consider a sphere containing uniform charge density $\rho = 3Ne/4\pi a^3$, the stress due to electrical forces on a plane through the center may be calculated by elementary means. If we demand that this stress be less than the tensile strength τ of the grain material we may write

$$\psi \leq \psi_D \equiv \frac{ae}{kT}\left(\frac{16\pi\tau}{3}\right)^{1/2} \sim \frac{500}{T_4} . \tag{25}$$

In graphite the value of τ depends on the direction in which force is applied with a minimum value of about 5×10^8 dyn cm^{-2}. Exposure to radiation somewhat increases the mechanical strength of graphite (Reynolds 1966). We have taken $\tau \sim 10^9$ dyn cm^{-2} as a reasonable estimate.

With ψ_D plotted in figure 3 we may see that mechanical disruption is important for $a = 0.1\ \mu$ in the temperature range $6 \times 10^3 \lesssim T_4 \lesssim 10^5$ where capture of positive nuclei is the important charging mechanism, but that for higher temperatures charging by secondary emission is not sufficient to destroy the grains. Thus in applications some care must be taken as the temperature history of the medium will have implications for the distribution of grain sizes. We discuss the effect of grain size in the following section.

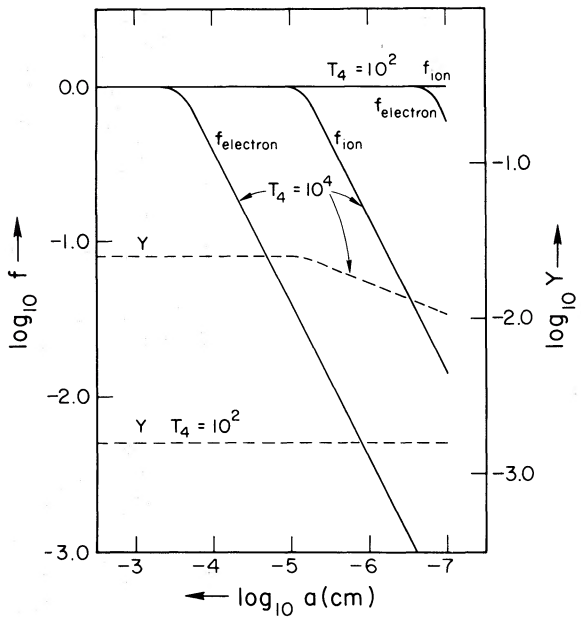

FIG. 4.—Fractional energy transfer per collision f_i and sputtering yield per collision Y versus grain radius a for two temperatures: $T_4 = 10^2$ and 10^4.

V. GRAIN PROPERTIES AS A FUNCTION OF RADIUS

In an astrophysical setting we may expect grains to be distributed over a spectrum, perhaps quite broad, of sizes. Furthermore, as the results of the last section indicate that grains of 0.1 μ radius may be mechanically destroyed, it is of interest to ascertain whether the fragments of a disrupted grain might themselves survive. In order to illustrate the dependence of grain properties on their radius, we present in this section detailed calculations for two temperatures, and we comment further on behavior at other temperatures.

a) Low Temperature: $T_4 = 10^2$

Sputtering interactions at this temperature are well described by Wehner's semiempirical formula and are of the nature of single-particle hard-sphere collisions. Sputtering then occurs very near the surface and is independent of grain radius (see fig. 4). Much the same is true for energy transfer by positive ions. Electrons, on the other hand, have a range against ionization losses of $\sim 2 \times 10^{-7}$ cm at this temperature and thus will have $f \propto a$ for radii less than that value.

The charge parameter ψ will have the Spitzer value for large radii. The electric field strength F at the grain surface set up by a given charge N is proportional to Na^{-2}, however, and we find that the charge at which field emission sets in is $N_{fe} \propto a^2$. Thus $\psi = Ne^2/akT \propto a$ for small radii as shown in figure 5.

The collisional energy input h is obtained according

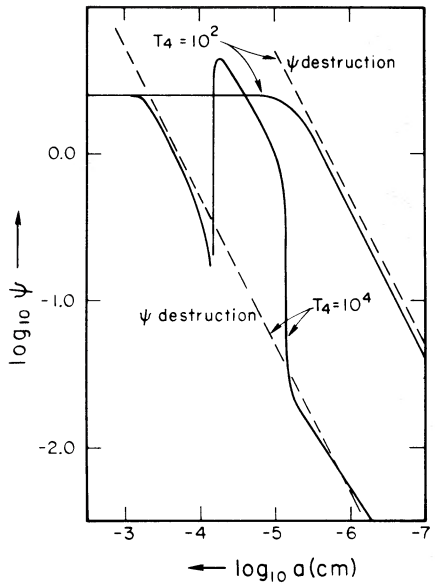

FIG. 5.—Grain charge ψ and its mechanical disruption limit $\psi_{\text{destruction}}$ versus grain radius a for two temperatures: $T_4 = 10^2$ and 10^4.

to the formula appropriate for negative charge:[1]

$$h \equiv h_0(T) f a\,, \tag{26}$$

where

$$f = \left[f_{\text{ion}}(1 + \psi + \psi^2/2) + \left(\frac{m_p}{m_e}\right)^{1/2} f_{\text{electron}}\, e^{-\psi} \right] \cdot \tag{27}$$

For large radii, f_{ion}, f_{electron}, and ψ are constant, so that $h \propto a^2$. For small a, however, the decrease in ψ first causes an increase in the contribution of electrons to f which is offset for yet smaller a by a decrease in f_{electron}. This behavior is graphed in figure 6.

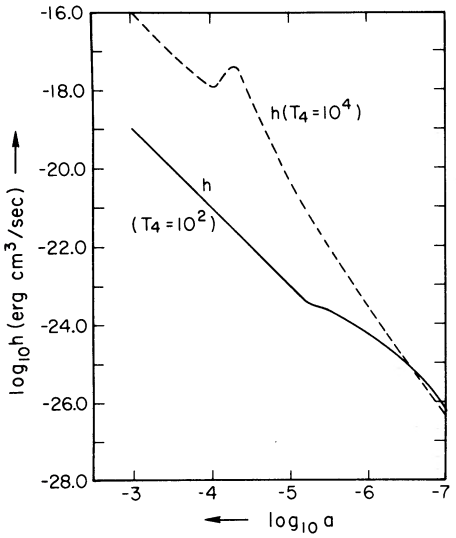

FIG. 6.—Collisional energy input for unit density h versus grain radius a for two temperatures: $T_4 = 10^2$ and 10^4.

[1] The quantity h is formally defined in equation (29) below: $h_0(T)$ is defined by equation (26).

b) *High Temperature:* $T_4 = 10^4$

At this temperature, ionization is the primary mechanism for energy transfer by positive ions as well as by electrons. Consequently, particles of both signs show similar behavior to that exhibited by electrons at $T_4 = 10^2$.

For sputtering, the Rutherford scattering calculation is approximately valid. For large radii, the range of knock-on carbon atoms inside the grain is less than the grain radius, and sputtering occurs primarily on entry and exit of the impinging particle. Sputtering is largely independent of grain radius in this regime. (We may expect a decrease by a factor 2 for radii greater than the range of the impinging particle, however, since the particle does not exit; we do not show this effect in fig. 4.)

For grain radii smaller than the range of knock-ons, particles may be sputtered from anywhere in the grain. However, the total number of particles so disturbed now depends on the radius of the grain and thus decreases for small radius as shown in figure 4.

The behavior of the charge parameter ψ now shows three distinct regimes (fig. 5). For the largest radii, the range of electrons is still less than grain size, so that the play-off between charge accretion and field emission is evident. In the intermediate regime, positive charge is accumulated by accretion. The limit set by the Stark effect is larger than the set by mechanical disruption throughout this regime, and we must conclude that grains of sizes $-5.2 \leq \log_{10} a \leq -4.2$ cannot survive for times $\gtrsim 10^7 n^{-1}$ s at this temperature. For the smallest values of a, ψ is fixed by an equilibrium between charge losses due to secondary electron emission and sputtering. As may be seen from figure 5, there is a small range of grain radius for which $\psi < \psi_{\text{destruction}}$, so that grains (or fragments of initially larger grains) (or fragments of initially larger grains) in this size range may survive.

The curve for h at $T_4 = 10^4$ shown in figure 6 is computed from equation (26) ignoring any grain disruption. The behavior for the very largest radii is $h \propto a^2$ and is appropriate for f_{ion}, f_{electron}, and ψ constants. For the smallest radii, $h \propto a^3$ since $\psi \sim 0$, f_{electron} is negligible, and $f_{\text{ion}} \propto a$. The peak at intermediate radii corresponds to the peak in ψ computed from the Stark effect. A large positive charge greatly increases the number of electron collisions. Of course, because of grain disruption, this peak is an ephemeral feature.

c) *Extrapolation to Other Temperatures*

The behavior of grain properties at $T_4 = 10^2$ is typical of lower temperatures, and extrapolation is relatively straightforward. Sputtering will become completely negligible for $T_4 \lesssim 30$ since incident-particle energies are then less than the sputtering threshold. Since $\psi_{\text{field emission}}$ and $\psi_{\text{destruction}}$ both vary as $\psi \propto aT^{-1}$, it is straightforward to scale figure 5 to lower

temperatures. Furthermore, we see that grain disruption does not occur whenever grain charge is limited by field emission.

For temperatures larger than $T_4 = 10^4$, we may scale values for f by noting that ionization losses vary roughly reciprocally with the energy of the incident particle; thus $f \propto T^{-2}$, and the graphs in figure 4 may be scaled accordingly.

There is no simple rule for scaling the sputtering. Rather we must consider how each feature of the graph of Y versus a changes with temperature. The value of a at which the graph for sputtering changes slope equals the range of the maximum energy knock-on produced by an incident particle of temperature T. Since the maximum energy of a knock-on is a fixed fraction of the incident particle energy and the range of a knock-on varies approximately as $\epsilon^{0.8}$, we have for the radius at which the slope changes $a_{\rm crit} \propto T^{0.8}$. Scaling of the value of Y on the flat portion of the plot of Y versus a at $T_4 = 10^4$ (where grain radius is greater than the maximum knock-on range) depends on the variation of the spectrum function $d\mathcal{N}(E)/dx$, the range $R(\epsilon)$, and the damage function $\nu(E)$ in a non-simple way. As may be seen in figure 2, the scaling is approximately $Y_{\rm flat} \propto T^{-0.8}$. The value of Y on the inclined portion of the curve in figure 4 depends only very weakly on variables other than the spectrum function and the energy at which knock-on range equals grain radius (not dependent on temperature). Thus $Y_{\rm inclined} \propto d\mathcal{N}(E)/dx \propto T^{-1}$.

Scaling of the graph for ψ may also be performed feature by feature. The boundaries of the three regimes are determined by the ranges of electrons and positive ions; thus $a_{\rm boundaries} \propto T$. Values of $\psi_{\rm field\ emission}$ and $\psi_{\rm destruction}$ scale readily as described above: $\psi \propto aT^{-1}$. Referring to equation (20) and (24) and recalling that Y varies approximately as T^1 for small grain radii, we may see that the same scaling is also *roughly* correct for $\psi_{\rm field\ emission}$ and $\psi_{\rm secondary\ emission}$. Thus the qualitative features of figure 5 are independent of temperature; the entire graph slides as a whole toward larger radii as temperature increases.

We have discreetly avoided mention of interpolation for temperatures $10^2 < T_4 < 10^4$. Here neither the semiempirical approach nor the Rutherford scattering approximation gives good results, and we have so far proceeded by graphical interpolation. Sensible numbers in this interval can probably be obtained by judicious use of the above extrapolation rules applied from both directions.

VI. GRAIN TEMPERATURES AND LIFETIMES

a) *Grain Temperature*

We now proceed to apply the preceding results in order to derive expressions for grain temperatures and lifetimes. The rate at which grains gain energy via gas atom collisions is

$$H_{\rm coll} = n_g \sigma_g \Sigma Q_i n_i \tfrac{1}{2} m_i \langle v_i^3 \rangle f_i \,, \tag{28}$$

where n_i, m_i, and v_i are the particle density, mass per particle, and random velocity of the ith type of particle, n_g and σ_g are the grain density and geometrical cross-section, and Q_i is the ratio of actual cross-section to σ_g for particles of the ith type. The summation is over all types of particles, including electrons. In order to make numerical estimates, we shall assume specific grain parameters appropriate for a graphite model grain, $\sigma_g n_g = 3 \times 10^{-22} n$ cm^2, radius $a = 0.1\ \mu$, and number of (heavy) atoms in the grain $N_a = 3 \times 10^8$.

With the results for the grain charge derived in § IV, we may now compute collision rates and fold them with the results of §§ II and III to obtain the total energy input rate per unit volume hn^2 ergs cm^{-3} s^{-1} and the total sputtering rate per unit volume Sn^2 cm^{-3} s^{-1}. We have plotted the quantities h and S as functions of T_4 in figure 3.

In the regime where field emission and photoemission are unimportant, we find that in an ionized medium of temperature T_4 ($\equiv T/10^4$ ° K),

$$H_{\rm coll} \equiv hn^2 = 1.1 \times 10^{-21} T_4^{3/2} n^2 f \text{ ergs cm}^{-3}\text{ s}^{-1} . \tag{29}$$

In this expression, we have introduced a new parameter f, the net energy transfer rate, which is defined to be

$$f = \frac{\sum_i Q_i n_i \frac{1}{2} m_i \langle v_i^3 \rangle f_i}{n \frac{1}{2} m_p \langle v_p^3 \rangle} ,$$

and is shown in figure 1 labeled "standard composition."

This may be compared with the rate of grain heating by absorption of radiation,

$$H_{\rm rad} = c n_g \sigma_g \langle Q_{\rm rad} \rangle U_{\rm rad} = 1.1 \times 10^{-23} n \langle Q_{\rm rad} \rangle \text{ ergs cm}^{-3}\text{ s}^{-1} , \tag{30}$$

where $\sigma_g \langle Q_{\rm rad} \rangle$ is the absorption coefficient averaged over the radiation field. In obtaining the numerical value, the interstellar radiation field has been used for the radiation density $U_{\rm rad}$.

Since $\langle Q_{\rm rad} \rangle$ may be as low as 0.01 for graphite or silicate particles, it is apparent that at high temperatures ($T \gg 10^5$ ° K) or high densities ($n \gg 1$ cm^{-3}), gas collisions can provide the dominant heat input for the grains.

Grain cooling occurs primarily by reradiation in the infrared. We write the absorption efficiency at infrared frequencies in the form

$$Q_{\rm rad}^{\rm (ir)} = C_1 (a\nu/c)^\alpha , \tag{31}$$

and find that the grain cooling rate can be expressed as

$$\Lambda_{\rm grain} = 4\pi n_g \sigma_g \int_0^\infty Q_{\rm rad} B_\nu(\nu, T_g) d\nu = 8\pi n_g \sigma_g h c^{-2} (a/c)^\alpha (kT_g/h)^{4+\alpha} C_2(\alpha) . \tag{32}$$

Here we have written

$$C_2(\alpha) = C_1 \Gamma(\alpha + 4) \zeta(\alpha + 4) .$$

Typically, we expect $\alpha \approx 1$ and $C_1 \approx 4$, so that

$C_2(1) = 100$. Inserting these numerical values, we find that

$$\Lambda_{\rm grain} = 3.8 \times 10^{-19} n(T_g/100^\circ\,{\rm K})^5\ {\rm ergs\ cm^{-3}\ s^{-1}}\ . \quad (33)$$

In the regions of interest, the corresponding grain temperature is given by equating $\Lambda_{\rm grain}$ and $H_{\rm coll}$:

$$T_g = 48(fn)^{1/5} T_4^{3/10}\ ^\circ{\rm K}\ . \quad (34)$$

b) *Grain Lifetimes*

Above the sputtering threshold, we write the grain lifetime against destruction by sputtering as

$$t_{\rm gr} \equiv \frac{n_g}{Sn_g^2} = [\langle v\rangle n\sigma_g Q_{\rm coll}]^{-1} N_a Y^{-1}$$
$$= 6.25 \times 10^{11} (YnT_4^{1/2})^{-1}\ {\rm s}\ . \quad (35)$$

Note that the threshold for sputtering graphite grains is about 50 eV per particle, or equivalent to a gas temperature of some 4×10^5 ° K. Hence graphite grains should indefinitely survive gas collisions at lower temperatures.

VII. CONCLUSIONS

We have described a general method which enables one to calculate the energy transfer to, and lifetimes of, interstellar grains in a hot gas. Specifically, our results for f and Y (figs. 1 and 2) and our general cooling and sputtering rates (fig. 3) refer to spherical graphite grains. It is relevant to comment here on the effect on our results of differing grain composition.

We assume the grain constituent atoms to have charge Z and atomic weight A; in a mixture of different substances, the following approximate results would be weighted proportionately. From figure 1, it is apparent that at gas temperatures below $\sim 10^7$ ° K the net rate f of energy transfer per grain encounter depends primarily on grain geometry, and will therefore be relatively insensitive to grain composition. Between 10^7 ° and 10^9 ° K, ionization losses of impinging particles become important, but depend only weakly (approximately logarithmically) on the ionization potential of the grain constituents. Above 10^9 ° K, the ionization losses vary approximately as Z.

We estimate that the threshold for normal sputtering of silicates is in the vicinity of 30 eV (cf. Stuart and Wehner 1962). For materials of comparable binding energy, such as graphite or silicates, the sputtering threshold would be expected in the simple sputtering model of § III to vary approximately as A^{-1}. Furthermore, as has been remarked above, the sputtering rate is relatively insensitive to the value of this threshold.

Above threshold, in the regime where the hard-sphere approximation is appropriate, the sputtering rate Y has a similar dependence on target-particle mass. However, at high temperatures, in the Rutherford scattering regime (at $T \geq 10^8$ ° K), Y varies approximately as Z^2A^{-1} (although this factor may be slightly reduced because of the reduction in path length for increased Z due to a larger rms scattering per encounter.

From these qualitative remarks it is apparent that our main results should not be grossly affected by consideration of different models of grain composition. From our more detailed discussion of the effects of grain size it is also clear that the distribution of grain sizes should not be of major importance to our conclusions. Indeed, our considerations of electric charge as a function of grain size and temperature could be used to draw rough conclusions about the size distribution in any given temperature regime.

Let us finally emphasize that our discussion of the physics of the interaction of interstellar grains with a hot gas is meant to provide a necessarily crude description of a regime that has not hitherto been studied. *Grains can survive in a hot gas, and may play an important role in the cooling of the gas and produce an appreciable amount of infrared radiation.*

We wish to thank M. Barlow, D. Gilra, J. P. Ostriker, E. M. Purcell, and E. E. Salpeter for stimulating discussions on topics relevant to this work. In particular, Michael Barlow provided a number of invaluable suggestions and references for the section on sputtering. The research of J. Silk has been supported in part by NASA grant NGR 05-003-453.

REFERENCES

Aannestad, P. 1971, unpublished Ph.D. thesis, University of California, Berkeley.
Barlow, M. 1971, *Nature Phys. Sci.*, **232**, 152.
Bruining, H. 1938, *Phillips Tech. Rev.*, **3**, 80.
Cox, D. D., and Tucker, W. H. 1969, *Ap. J.*, **157**, 1157.
Eggen, D. T. 1950, USAEC Report NAA-SRO-69.
Feuerbacher, B., Willis, R. F., and Fitton, B. 1973, *Ap. J.*, **181**, 101.
Gomer, R. 1961, *Field Emission and Field Ionization* (Cambridge: Harvard University Press).
Habing, H. J. 1968, *B.A.N.*, **19**, 421.
Henschke, E. B. 1962, *J. Appl. Phys.*, **33**, 177.
KenKnight, C. E., and Wehner, G. K. 1964, *J. Appl. Phys.*, **35**, 322.
Lucas, M., and Mitchell, A. 1964, *Carbon*, **1**, 345.
Mathews, W. G. 1969, *Ap. J.*, **167**, 583.
Mott, N. F., and Massey, H. S. W. 1933, *The Theory of Atomic Collisions* (Oxford: Clarendon Press), p. 169.
Ostriker, J. P., and Silk, J. 1973, *Ap. J. (Letters)*, **184**, L113.
Pecker, J. C. 1971, *C.R. Acad. Sci. Paris*, **272**, 69.
Reynolds, W. N. 1966, *Chemistry and Physics of Space*, Vol. **2**, ed. Walker (New York: Marcel Dekker), p. 121.
Rosenberg, D., and Wehner, G. K. 1962, *J. Appl. Phys.*, **33**, 1842.
Silk, J., and Burke, J. R. 1974, *Ap. J.*, **190**, 11.
Spitzer, L. 1941, *Ap. J.*, **93**, 369.
Spitzer, L. 1968, *Diffuse Matter in Space* (New York: Interscience), p. 145.
Stuart, R. V. 1961, *Trans. 8th National Vacuum Symposium*, Vol. **2** (London: Pergamon), p. 252.
Stuart, R. V., and Wehner, C. K. 1962, *J. Appl. Phys.*, **33**, 2345.
Thompson, M. W., and Wright, S. B. 1965, *J. Nucl. Matter*, **16**, 146.
Venables, J. A. 1970, *Atomic Collision Phenomena in Solids*, ed. D. W. Palmer, M. W. Thompson, and P. D. Townsend (Amsterdam: North-Holland), pp. 132–161.
Watson, W. D. 1972, *Ap. J.*, **176**, 103.
Wehner, G. K. 1958, *Phys. Rev.*, **112**, 1120.
Wehner, G. K., KenKnight, C. D., and Rosenberg, D. 1963, *Planet. and Space Sci.*, **11**, 1257.
Wickramasinghe, N. 1972, *M.N.R.A.S.*, **159**, 269.
Zel'dovich, Ya. B., and Raizer, Yu. P. 1967, *Physics of Shock Waves and High Temperature Hydrodynamic Phenomena*, Vol. **2** (New York: Academic Press), pp. 716–721.